

# Strain Rate Effects in the Mechanical Response of Polymer-Anchored Carbon Nanotube Foams

By Abha Misra, Julia R. Greer, and Chiara Daraio\*

Super-compressible foam-like carbon nanotube films<sup>[1–7]</sup> have been reported to exhibit highly nonlinear viscoelastic behavior in compression similar to soft tissue.<sup>[4]</sup> Their unique combination of light weight and exceptional electrical, thermal, and mechanical properties have helped identify them as viable building blocks for more complex nanosystems and as stand-alone structures for a variety of different applications. In the as-grown state, their mechanical performance is limited by the weak adhesion between the tubes, controlled by van der Waals forces, and the substrate allowing the forests to split easily and to have low resistance in shear.<sup>[5]</sup> Under axial compression loading carbon nanotubes have demonstrated bending, buckling,<sup>[8]</sup> and fracture<sup>[9]</sup> (or a combination of the above) depending on the loading conditions and the number of loading cycles.<sup>[4]</sup> In this work, we study the strain rate effects on the mechanical properties of carbon nanotube forests and report several related interesting new phenomena. We partially anchor<sup>[10]</sup> dense vertically aligned foam-like forests of carbon nanotubes on a thin, flexible polymer layer to provide structural stability, particularly at the higher strain rates. The goal of the anchoring was also to create versatile nanosystems, which integrate the excellent nanotube properties in a light-weight portable system. We test the sample under quasi-static indentation loading and under impact loading and report a variable nonlinear response and different elastic recoveries with varying strain rates. A Bauschinger-like effect is observed at very low strain rates while buckling and the formation of permanent defects in the tube structure is reported at very high strain rates. Using high-resolution transmission microscopy we observe for the first time the delamination and crumbling of carbon nanotube walls. These polymer-anchored CNT foams are reported to behave as conductive nanostructured layers, suitable as fundamental building blocks for a variety of different applications, or as new self-standing application-ready materials with potential employment as actuators, impact absorbers, or as layered components for the creation of acoustic dampers.

Because of the excellent thermal, electronic and mechanical properties, vertically aligned carbon nanotube (CNT) arrays have been proposed for several potential applications, ranging from biomimetic adhesives similar to spider's and gecko's feet,<sup>[11]</sup> to nanobrushes,<sup>[12]</sup> vibration damping layers,<sup>[6]</sup> and multifunctional composites,<sup>[13]</sup> but their development into successful commercial applications has been limited by their weak adhesion to the growth substrate, resulting in poor resistance to shear. In the present work we grew long, vertically-aligned multiwall CNTs (Fig. 1a), transferred and anchored them in thin polymer layers (Fig. 1b), and tested their mechanical response. While the nanotubes appear to be vertically aligned throughout the entire thickness of the sample (Fig. 1b), scanning electron microscopy (SEM) images taken at higher magnifications (Fig. 1b, upper inset) reveal a much more complex microstructure with nanotubes entangled in an open foam-type cellular matrix<sup>[15]</sup> throughout the thickness. In addition, previous investigations of cyclic compressive loading of CNT foams<sup>[3]</sup> reported that such structures have a slightly anisotropic mechanical response between the tip and the base of the tubes, with the base part being more prone to buckling (and therefore more inclined to demonstrating a softer, nonlinear response) due to a lower overall density. Our anchoring method is designed to embed only the tips of the tubes into the polymer,<sup>[10]</sup> leaving the bases exposed to the indenter or a ball contact during mechanical testing and therefore maximizing sample compliance and observed nonlinear effects. A zoomed-in view of the thin polymer anchoring layer is provided in the lower inset of Fig. 1b.

Flat punch indentations (Fig. 2) and drop-ball impact tests (Fig. 3) were performed to characterize their quasi-static and dynamic response in compression. Indentation measurements (Fig. 2a) were obtained using a flattened (by focus ion beam) Berkovich diamond punch ( $\sim 30\ \mu\text{m}$  diameter). The load–displacement data curves are presented in Fig. 2b. It is evident from the curves that there are three distinct regions upon loading, most likely related to densification, bending, and buckling modes of the nanotubes immediately under the indenter. This nonlinear behavior is qualitatively similar to the viscoelastic properties reported for tests of single attached myoblast cells under compression<sup>[14]</sup> and soft open foams.<sup>[15]</sup> We report that the amount of elastic recovery is inversely proportional to the indentation depth (varying between 10% and 25% in the tested range). The load–displacement curves were analyzed using the flat punch/infinite medium contact analysis method developed by Sneddon<sup>[16]</sup> with the projected area of compression being that of the nanoindenter flat punch. Assuming a purely uniaxial compression we plotted normal stress–strain curves with varying loading/unloading cycles. For example, Figure 2c shows that the foams were unloaded to  $\sim 10\%$  of the maximum load and subsequently reloaded at strains of  $0.75 \times 10^{-4}$  and  $1.5 \times 10^{-4}$ . It

[\*] Prof. C. Daraio  
Graduate Aeronautical Laboratories (GALCIT), and Applied Physics  
California Institute of Technology  
Pasadena, CA, 91125 (USA)  
E-mail: daraio@caltech.edu

Prof. J. Greer  
Materials Science and Mechanical Engineering  
California Institute of Technology  
Pasadena, CA, 91125 (USA)

Dr. A. Misra  
Graduate Aeronautical Laboratories (GALCIT)  
California Institute of Technology  
Pasadena, CA, 91125 (USA)

DOI: 10.1002/adma.200801997

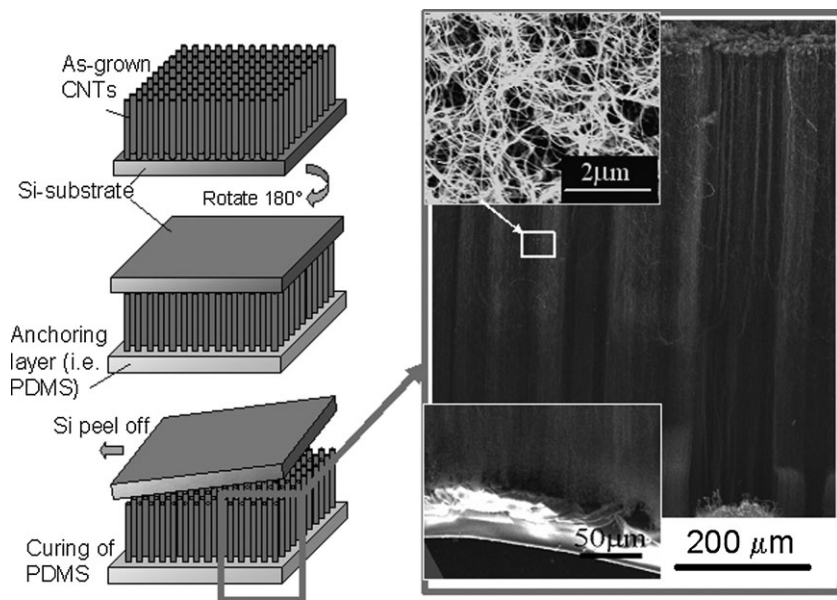


**Figure 1.** Synthesis and assembly of the transportable polymer-anchored CNT foams. a) Schematic diagram showing the growth and anchoring steps for the CNT forests. b) SEM image of the nanotube films showing the foam microstructure. Top inset shows a higher magnification image of the nanotubes. Bottom inset is a zoomed-in image of the polymer anchoring layer. The nanotube tips are embedded in the polymer going fully through the polymer thickness as confirmed by electrical measurements.

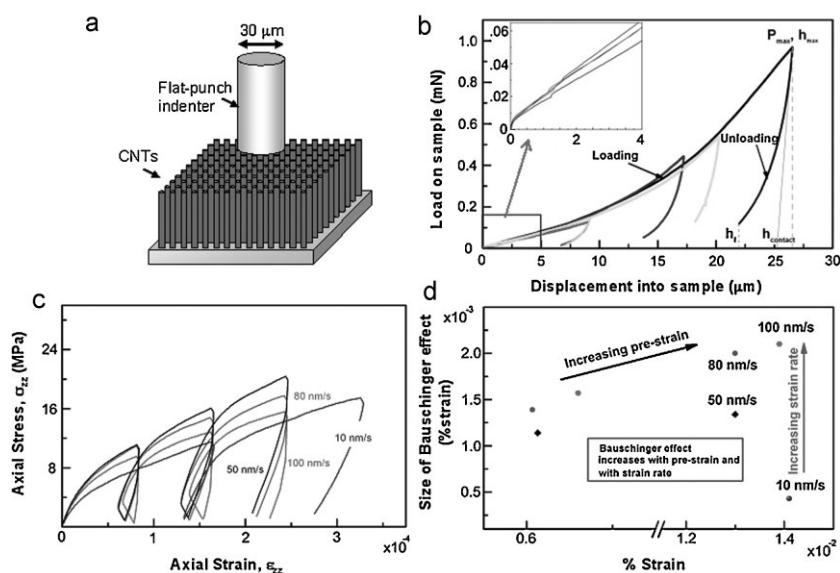


**Figure 2.** Flat punch nanoindentation results. a) Schematic diagram showing the experimental set up. b) Load–displacement curves obtained at different loading rates. c) Stress–strain curves extrapolated by the indentation measurement at varying strain rates upon various loading/unloading cycles showing the presence of a Bauschinger-like effect. d) Dependence of the hysteresis loop amplitude on strain.

is very interesting to notice that the nanotube foams consistently exhibit hysteresis, or Bauschinger-like effect, during these unloading/reloading paths. The Bauschinger effect (similar to the Mullins effect in rubber) refers to a property of materials where the stress–strain characteristics change as a result of the

microscopic stress distribution. To quantify the strain rate effects on the hysteretic response we plotted the size of the Bauschinger effect as a function of strain. It is evident that the hysteresis increases proportionally to both the pre-strain and the strain rate. We explain this phenomenon by the local densification effects directly below the compressed area. This finding is consistent with the previous reports of the viscoelastic compressive response and densification effects in free-standing, non-anchored structures under uniform applied stress.<sup>[4]</sup>

To evaluate the high strain rate response of the polymer-anchored foams, we performed drop-ball impact tests while systematically varying the impact velocity. Results related to the highest impact velocity ( $4 \text{ m s}^{-1}$ ) are reported in Figure 3. Such impact velocity roughly corresponds, for example, to the drop of an electronic device (i.e., cell phone, remote, or personal computer) from the average height of a table or shelf. From the Force ( $F$ )–time ( $t$ ) responses reported in Figure 3b it is evident that the anchored nanotube forest works efficiently as an impact absorber and a pulse mitigation layer, suggesting its applicability as a free-standing protective layer in microelectronic packaging. To show their effectiveness we compare the impact mitigation performance of the polymer-anchored CNTs (curve 3) with the same impact performed on a single layer of polymer with no nanotubes ( $\sim 50 \mu\text{m}$  thick, curve 1) and on an as-grown CNT forest on a Si substrate (curve 2). Note also that in the latter the nanotube forest is flipped upside down (with tips headed up) with respect to the anchored layer reported in curve 3. The difference reported here is also striking when comparing the Force ( $F$ )–displacement ( $\delta$ ) response under impact. These curves are constructed by integrating two times the measured  $F$ – $t$  response and from knowing the initial and final impact velocity of the striker.<sup>[6,7,9]</sup> The distinct response of the nanotube foams upon tip or base impact is evident (compare curves 2 and 3 in Fig. 3c), showing a more pronounced nonlinear response in the latter.

We evaluated the recovery and permanent deformation damage by using SEM and transmission electron microscopy (TEM) (Fig. 4). The effect of the flat indentation tests on the surface of the foam-like forests of CNTs

is shown in Figure 4a. The inset highlights a cross-sectional view, etched with a focused ion beam, of the nanotube foam below the indenter mark. The bending and the densification of the initially uncompressed open nanotube foam are evident. The diameter of the circular indentation mark is  $\sim 30 \mu\text{m}$ , which matches exactly

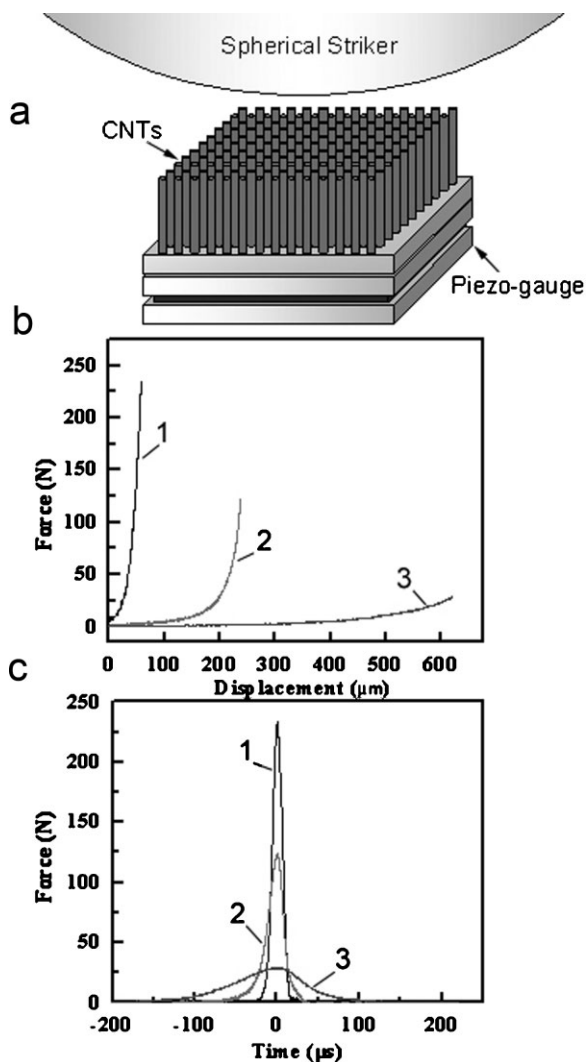


**Figure 3.** Impact (high strain rate) results. a) Schematic diagram showing the experimental set-up. (b)  $F$ - $\delta$  curves obtained impacting a stainless steel bead at  $\sim 4 \text{ m s}^{-1}$  on a single PDMS layer (curve 1), an as-grown CNT forest on a Si substrate (curve 2), and on our PDMS-anchored CNT forest (curve 3). c)  $F$ - $t$  response measured experimentally for the same impacts.

the area of the cylindrical indenter. The impact area ( $\sim 1 \text{ mm}$  in diameter) after a  $4.0 \text{ m s}^{-1}$  drop-ball test is reported in Figure 4b. In light of the large deformations reported in the  $F$ - $\delta$  behavior (Fig. 3c) it is evident that the nanotube foam is capable of a very large spring-back recovery (from a maximum compression of  $\sim 600 \mu\text{m}$ ), leaving the surface of the film only partially damaged. The maximum local pressure in the impacted area has been calculated at  $\sim 60 \text{ MPa}$ . Such high stresses are likely to cause locally permanent damage to the tubes, which we investigated via high resolution TEM (FEI TF30U). Figure 4c shows the microstructure of a typical undamaged, as-grown carbon nanotube in the forest. The effects of the high impact velocity ( $4.0 \text{ m s}^{-1}$ ) on the buckled tubes are reported in Figures 4d and e. We noticed two different types of permanent damage of the structure: in addition to the previously reported bending and rippling<sup>[17]</sup> of the tubes (Fig. 4e) we discover a new effect of

delamination and crumbling of the inner walls of the tubes (Fig. 4d), possibly related to the confining effect along the radial direction provided by the presence of neighboring nanotubes upon impact. To the best of our knowledge this represents the first experimental report of such dynamically generated defects and challenges some of the classical theoretical and numerical predictions of carbon nanotube deformation at high strain rates, opening up new avenues for computational studies.

We also investigated the electrical properties of the anchored nanotube foams by monitoring the conductivity of the foams in the in-plane and the cross-sectional orientation (including the intrinsically insulating PDMS anchoring layer). Interestingly the conductivity values obtained in both directions were very similar: it was measured to be  $0.42 \text{ Scm}^{-1}$  at the tangled foam surface, and  $0.16 \text{ Scm}^{-1}$  along the cross section. These results demonstrate that the CNTs go through the polymer layer leaving most of their tips exposed on the opposite side. Such polymer/CNT composites present a cross-sectional conductivity value only slightly lower than the previously reported value for a free standing CNT forest (with no substrate anchoring).<sup>[4]</sup> This opens up a myriad of applications ranging from nanoactuators to chemical separator membranes and sensing devices.<sup>[18]</sup>

In conclusion, anchored foam-like forests of carbon nanotubes were found to demonstrate a highly nonlinear dynamic response when subjected to mechanical impact as well as excellent energy absorption capabilities. At small strain rates (on the order of  $10^{-8} \text{ s}^{-1}$ ) the response of the anchored foams appears to be elastic/plastic with the hysteretic loading/unloading response sensitive to the variation in the strain rate. At higher strain rates ( $10^3$ - $10^4 \text{ s}^{-1}$ ) and axial loads, the formation of permanent defects in the multiwalled structure of the CNTs in the foam is reported and suggests new modes of deformation related to the delamination of tube cores. These results suggest that foam-like forests of CNTs strongly anchored in thin polymer layers form hybrid structures between pure CNT forests and CNT composite films<sup>[19]</sup> with significantly enhanced properties over their individual components, providing a viable engineering solution for lightweight, small shock absorbers and impact protective layers for electronics and space applications.

## Experimental

**CNT Growth and Anchoring:** The arrays of multiwalled carbon nanotubes were grown on Si substrates using a two-stage thermal chemical vapor deposition (CVD) system. The solution of catalyst (ferrocene) and carbon source (toluene) was heated at  $825 \text{ }^\circ\text{C}$  in a long quartz tube in the presence of argon flow as carrier gas. The length of the grown forest was  $\sim 800 \mu\text{m}$  and its density was estimated at  $\sim 100 \text{ CNTs } \mu\text{m}^{-2}$ . A rapid transfer method from the growth substrate to the thin polymer layer has been employed. Poly(dimethylsiloxane) (PDMS) was spin-coated on top of the glass slide at  $800 \text{ rpm}$  to get a  $\sim 50 \mu\text{m}$  thick film. The CNT forests could then be anchored on top of the polymer surface. The polymer was cured after partial infiltration at  $80 \text{ }^\circ\text{C}$  for 1 h, after which the anchored films were peeled off the glass slide. The advantage of this method is that the geometry of the nanotube network can be predetermined by the growth conditions in the CVD chamber. The forests of CNTs studied in this work presented a very interesting microstructure. A very good vertical alignment was evident at a macroscopic scale, where bundles of CNTs were clearly growing parallel to each other. At a smaller

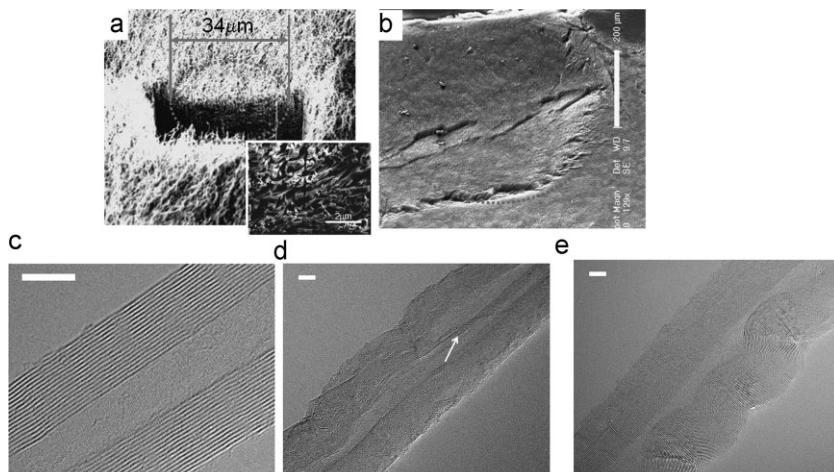


**Figure 4.** Characterization of the deformed forests. a) SEM image obtained on the surface of the sample after flat indentation tests and FIB slicing. The inset shows a closer view of the compressed cross-sectional area underneath the indenter. b) Tilted top view of the damaged area on the CNT-foam surface after  $\sim 4 \text{ m s}^{-1}$  impact (marked by circle). c) High resolution TEM image of a typical as-grown CNT. d) TEM image of a permanently deformed CNT showing delamination and crumbling of the walls. e) TEM image of rippled and buckled nanotube. The scale bars for c–e are 5 nm.

scale the alignment appeared to be lost because the long single tubes tended to be less straight and more tangled with each other in the bundles.

**Flat indentation mechanical testing:** The tests were performed using the dynamic contact module (DCM) of the MTS Nanoindenter G200 with a flat punch indenter tip in continuous stiffness measurement (CSM) mode at room temperature, varying the displacement rate loading. The flat punch tip was custom fabricated from a standard Berkovich indenter by using the focused ion beam (FIB) to machine off the diamond tip, resulting in the projected area of a circle with a  $\sim 30 \mu\text{m}$  inscribed diameter. The MTS G200 Nanoindenter system is thermally buffered from its surroundings to within  $1^\circ\text{C}$ , however, small temperature fluctuations cause some of the machine components to expand and contract, and this thermal drift is corrected by monitoring the rate of displacement in the final 100 s of the hold period. Load–displacement data were collected in the CSM mode of the instrument. The experimental procedure involved first locating the area of choice under the top-view  $40\times$  optical microscope, then calibrating the indenter to microscope distance to within a fraction of a micrometer on the surface of the sample away from the selected position, and finally moving the calibrated flat indenter tip to the position directly above the selection. Thermal drift stabilization follows the compression of the foam at a constant nominal displacement rate. During the initial segment of the test, the instrument locates the sample surface and then moves to the specified location and starts the initial approach segment, decreasing the approach velocity to  $54 \text{ nm s}^{-1}$  when the indenter is less than  $2 \mu\text{m}$  above the surface. Once the surface of the CNT foam has been detected, such parameters as the load, or force, harmonic contact stiffness, and the compressive displacement of the surface from the point of contact are continuously measured and recorded.

**Impact testing:** The experimental setup used for high strain rate tests consisted of a benchtop system [5,6,8] that included a free-falling sphere (Bearing-Quality Aircraft-Grade 25, Alloy Chrome Steel precision stainless steel ball, diameter 4.76 mm, with a surface roughness (RA)  $\sim 50 \text{ nm}$  maximum, made from AISI type 52100 steel, McMaster-Carr cat.) and a calibrated piezosensor (Piezoelectric single sheet, T110-A4-602 provided by Piezo-System, Inc. with soldered 34 AWG microminiature wiring) connected to a Tektronix oscilloscope (TDS 2024B) to detect  $F-t$  curves. The use of a sphere, as opposed to a flat plate, allows the application of a reproducible large concentrated force so that each nanotube can be subjected to sufficient impact energy. The impact on the

aligned nanotubes was generated by dropping the 4.76 mm diameter steel sphere (0.45 g) from variable heights (0.5–80 cm), which correspond to a speed of impact of  $\sim 0.3\text{--}4 \text{ m s}^{-1}$ . Accordingly, the overall strain rate was calculated to be on the order of  $10^3\text{--}10^4 \text{ s}^{-1}$ .

**Polymer–CNT adhesion testing:** We have performed independent tension tests on doubly-anchored CNT forests (two PDMS layers were anchored on both the top and bottom of the forests) to evaluate the effective adhesion of the CNTs with the anchoring polymer layer. To ensure uniform gripping for the tests, the PDMS layers were first spin-coated on glass slides and then cured. We used a custom made tension/compression test system with a ALD-MINI-UTC-M 500 g load cell from A. L. Design. Tension test results showed consistently that the maximum normal tension force at failure was measured  $\sim 2.3 \text{ N}$  and in all cases failure always happened by the detachment of the PDMS polymer from the glass slide and never by debonding of the CNTs from the anchoring layer. These results are consistent with what was reported for similarly anchored CNTs in RTV layers [10] and confirm the excellent adhesion of the tubes with the thin substrate.

**Electrical testing:** Two-point electrical measurements were performed by using an Alessi REL-3200 probe station attached with Keithley-236 source measure unit system to evaluate the in-plane conductivity at the surface of the CNT arrays as well as along the tube lengths and through the anchoring PDMS polymer layer. A constant current (5 mA) was applied while the voltage was measured.

## Acknowledgements

C.D. and J.R.G. wish to acknowledge the support of this work by their Caltech start-up funds, A.M. acknowledges support by the Moore Fellowship. The authors also thank C. Kovalchick for his support on the CNTs/polymer adhesion tests and C. Garland on TEM supervision.

Received: July 15, 2008

Revised: September 10, 2008

Published online:

- [1] H. J. Qi, K. B. K. Teo, K. K. S. Lau, M. C. Boyce, W. I. Milne, J. Robertson, K. Gleason, *J. Mech. Phys. Solids* **2003**, *51*, 2213.
- [2] S. Dj, Mesarovic, C. M. Mccarter, D. F. Bahr, H. Radhakrishnan, R. F. Richards, C. D. Richards, D. McClain, J. Jiao, *Scr. Mater.* **2007**, *56*, 157.
- [3] A. Cao, P. L. Dickrell, W. G. Sawyer, M. N. Ghasemi-Nejhad, P. M. Ajayan, *Science* **2005**, *310*, 1307.
- [4] J. Suhr, P. Victor, L. Ci, S. Sreekala, X. Zhang, O. Nalamasu, P. M. Ajayan, *Nat. Nanotechnol.* **2007**, *2*, 417.
- [5] E. H. T. Teo, W. K. P. Yung, D. H. C. Chua, B. K. Tay, *Adv. Mater.* **2007**, *19*, 2941.
- [6] C. Daraio, V. F. Nesterenko, S. Jin, *Appl. Phys. Lett.* **2004**, *85*, 5724.
- [7] C. Daraio, V. F. Nesterenko, S. Jin, W. Wang, A. M. Rao, *J. Appl. Phys.* **2006**, *100*, 064309.
- [8] M. R. Falvo, G. J. Clary, R. M. Taylor, V. Chi, F. P. Brooks, S. Washburn, R. Superfine, *Nature* **1997**, *389*, 6651.
- [9] C. Daraio, V. F. Nesterenko, J. Aubuchon, S. Jin, *Nano Lett.* **2004**, *4*, 1915.
- [10] E. B. Sansom, D. Rinderknecht, M. Gharib, *Nanotechnology* **2008**, *19*, 035302.
- [11] B. Yurdumakan, N. R. Raravikar, P. M. Ajayanb, A. Dhinojwala, *Chem. Commun.* **2005**, 3799.

- [12] A. Cao, V. P. Veedu, X. Li, Z. Yao, M. N. Ghasemi-Nejhad, P. M. Ajayan, *Nat. Mater.* **2005**, *4*, 540.
- [13] V. P. Veedu, A. Cao, X. Li, K. Ma, C. Soldano, S. Kar, P. M. Ajayan, M. N. Ghasemi-Nejhad, *Nat. Mater.* **2006**, *5*, 457.
- [14] A. G. Erniel, E. A. G. Peeters, C. W. J. Oomens, C. V. C. Bouten, D. L. Bader, F. P. T. Baaijens, *J. Biomech. Eng.* **2005**, *127*, 237.
- [15] L. J. Gibson, M. F. Ashby, *Cellular Solids*, Pergamon Press, Oxford **1988**.
- [16] I. N. Sneddon, *Int. J. Sci. Eng.* **1965**, *3*, 47.
- [17] M. Arroyo, T. Belytschko, *Phys. Rev. Lett.* **2003**, *91*, 215505.
- [18] B. J. Hinds, N. Chopra, T. Rantell, R. Andrews, V. Gavalas, L. G. Bachas, *Science* **2005**, *303*, 62.
- [19] P. M. Ajayan, J. M. Tour, *Nature* **2007**, *447*, 1066.
-